LA-UR -87-4016

Los Alamos National Laboratory is operated by the University of California for the United States Department of Energy under contract W-7405-ENG-36

LA-UR--87-4016

DE88 004316

TITLE FURTHER CONSIDERATIONS OF CRITICAL HEAT FLUX IN SATURATED POOL BOILING DURING POWER TRANSIENTS

AUTHOR(S) Kemal O. Pasamehmetoglu and Ralph A. Nelson

SUBMITTED TO ASME/AIChE/ANS National Heat Transfer Conference
Houston, Texas
July 24-27, 1988

DISCLAIMER

MASTER

Los Alamos Los Alamos National Laboratory
Los Alamos, New Mexico 87545

FURTHER CONSIDERATIONS OF CRITICAL HEAT FLUX IN SATURATED POOL BOILING DURING POWER TRANSIENTS*

by

Kemal O. Pasamehmetoglu and Ralph A. Nelson

Safety Code Development
Nuclear Technology and Engineering Division
Los Alamos National Laboratory
Los Alamos, New Mexico 87545

ABSTRACT

In this paper, we further evaluate our previously postulated transient CHF model. First, we verify the steady-state CHF model on which the transient model is based by using recent macrolayer thickness data. We also include the effect of thermal storage in the heater that we previously neglected. The use of a simplified approach in the prediction of the instantaneous surface heat flux for given power generation rates considerably improves the predictive capability of the transient critical heat-flux (CHF) model. Finally, we discuss the statistical vapor mass behavior during transient boiling and its effect on the transient CHF model. We show that the data scatter within a small range may be partially explained through such an approach.

I. INTRODUCTION

Boiling heat transfer with time-dependent heat input, as well as the prediction of the critical heat flux (CHF) under such conditions, is of interest in several applications related to the safety of nuclear and chemical plants. One application in light water nuclear reactor technology involves the reactivity initiated accident (RIA), in which a sudden increase in power generation may occur. Therefore, accurate modeling of transient CHF is required to evaluate RIA scenarios.

In the past, there have been several experimental studies aimed at providing a fundamental understanding of the transient CHF phenomenon in saturated pool boiling [1-3]. Tachibana *et al.*[1] Sakurai *et al.*[2] and Kawamura *et al.*[3] measured the transient CHF using flat ribbon heaters of small sizes placed vertically in a pool of water at atmospheric pressure. Sakurai

* This work was funded by the US Nuclear Regulatory Commission (NRC), Office of Nuclear Regulatory Research, Division of Accident Evaluation.

and Shiotsu[4,5] used a horizontal platinum wire with a 1.2 mm diameter. They measured the transient CHF in saturated pool boiling at pressures ranging from atmospheric (0.1 MPa) to 2.0 MPa. The power to the heater was increased exponentially with a period ranging from 5 ms to 10 s.

The first comprehensive theoretical modeling of the CHF during power transients is presented by Serizawa.[6] Unfortunately, the model contradicts the physical evidence presented by other investigators. First, Serizawa's steady-state boiling model[6] is based upon a continuous liquid supply to the macrolayer. This assumption contradicts the saturated pool boiling model of Haramura and Katto,[7] which will be summarized in the following section. Secondly, the final quantification of Serizawa's model requires one of its important parameters, the macrolayer thickness, to be correlated empirically. This was done by directly comparing the model with transient CHF data. Therefore, a good agreement between the data and the model is not surprising. However, this empirically correlated magnitude of the macrolayer thickness is more than an order of magnitude smaller than that proposed by Haramura and Katto.[7] It is almost two orders of magnitude smaller than that measured by Bhat *et al.*[8] and Iida and Kobayasi.[9]

Recently, we proposed a new theoretical model[10] to correlate the transient CHF in saturated pool boiling. The physics of this new model is in agreement with the steady state CHF model of Haramura and Katto.[7] Furthermore, in addition to an evaporation mechanism, the new model also considers a hydrodynamic-thinning mechanism of the macrolayer for faster transients. The details of this model may be found in Refs. 10 and 11 and are not repeated here. The final transient CHF correlation was obtained in the following form for exponentially increasing surface heat flux

$$\eta \quad \{1 \quad H(B_s \quad 1)\}\left[1 \cdot \left(\frac{B_s^3}{2}\right)\right] \cdot 1.5\{H(B_s \quad 1)\}B_s \quad , \tag{1}$$

where

$$\eta \quad \frac{q_{CHF\_TR}}{q_{CHF\_SS}} \quad ,$$

and B_s is the switch over parameter defined as the ratio of the switch over heat flux to steady state CHF. The switch over heat flux is the heat flux at which the macrolayer thinning mechanism changes from hydrodynamic to thermal. The switch over parameter[10] for an exponential increase in the heat flux becomes

$$B \quad \left(\frac{2\tau_d}{\tau}\right)^{1/3} \quad , \tag{2}$$

where τ_d is the vapor mass (bubble) hovering period evaluated when the surface heat flux is equal to steady state CHF (see App. A) and τ is the exponential period of the surface heat flux.

In our previous study,[11] we compared Eq. (1) with the data of Sakurai and Shiotsu.[5] At high pressures, where the regular boiling occurs (as defined by Sakurai and Shiotsu[4,5]), the theory consistently overpredicts the fast transient data although the prediction is within 25%. However, this earlier publication does not contain a systematic and comprehensive evaluation

of the different parameters and assumptions affecting the final result. The major areas that require further discussion are as follows

1 The most recent macrolayer thickness data of Bhat *et al.*[6] may be used for a more direct verification of the steady state CHF model of Haramura and Katto.[7]

2 In our previous paper, in comparing the theory and the data, we assumed that the surface heat flux may be related to the heat generation rate through a simple volume to surface area ratio. Thus, we used the exponential period of the heat generation rate, τ, instead of the exponential period of the surface heat flux, τ^*. This approach obviously introduces some error during fast transients where thermal storage within the heater may become significant. The effect of this error on the data comparison must be quantified.

3. During transient boiling, it is impossible to account for the history of individual vapor masses. Thus, a statistical analysis of the final prediction must also be provided even though the range is expected to be relatively small.

4. In Eqs. (1) and (2), the vapor mass hovering period, τ_d, is calculated through the solution of the idealized bubble equation of motion as suggested by Haramura and Katto[7] and summarized in App. A. Such a purely analytical idealized approach is likely to introduce some error.

Items 1 through 3 are discussed in Secs. II through IV, respectively. The discussion of item 4 is not included in this paper because we do not have any new experimental or analytical evidence to re-evaluate the validity of the theoretically predicted magnitude of τ_d. Earlier, we showed that, if all the other parameters are assumed to be accurate, the error in evaluating τ_d is confined within 25% (see Ref. 10, Fig. 8). Finally, the summary and conclusions are presented in Sec. V

II. VERIFICATION OF THE STEADY-STATE MODEL

The multistep saturated pool boiling model of Haramura and Katto[7] assumes that, at high heat fluxes near CHF, the heater surface is crowded with hovering vapor masses. The bulk liquid reaches the heater surface only when the vapor mass departs. Consequently, CHF occurs if the heat flux is high enough to evaporate the total macrolayer under the vapor mass during its hovering (growth) period. Mathematically, this model yields the following expression for CHF,

$$\tau_d q_{CHF,SS} = \rho_f h_{fg} \delta_{max} \left(1 - \frac{A_v}{A_w}\right) , \tag{3}$$

where τ_d is the hovering period of the vapor mass and is given in App. A. The initial macrolayer thickness, δ_{max}, is postulated by Haramura and Katto[7] to be one fourth of the Helmholtz instability wavelength along the vapor stems. Thus,

$$\delta_{max} = \frac{\pi}{2^5} \sigma \left(\frac{\rho_f + \rho_g}{\rho_f \rho_g}\right) \left(\frac{A_v}{A_w}\right)^2 \left(\frac{\rho_f h_{fg}}{q_{CHF,SS}}\right)^2 , \tag{4}$$

where A_1/A_w is the ratio of the heater area covered by vapor to the total heater area. In this model, the parameter A_1/A_w was evaluated through an indirect approach by Haramura and Katto. They compared their model with the well known Zuber CHF correlation[12] (see App. B) in order to compute the parameter A_1/A_w. Obviously, such an approach invalidates the numerical assessment of the model against the CHF data.

Instead of this indirect approach, we evaluated the parameter A_1/A_w by directly comparing the Helmholtz instability model with the macrolayer thickness data of Bhat *et al.*[5] This comparison, which is discussed further in an earlier paper,[13] is not repeated here. It suggests that the macrolayer-thickness data at atmospheric pressure is best predicted if

$$0.0164 \le \frac{A_1}{A_w} \le 0.0220 \quad .$$

When these bounding values are substituted into Eqs. (3) and (4), the model of Haramura and Katto predicts the following range for CHF over a horizontal surface at atmospheric pressure.

$$1.251 \le q_{CHF,SS} \le 1.503 \ \ (\mathrm{MW/m^2}) \quad .$$

At atmospheric pressure, the Zuber correlation, described in App. B, yields 1.261 MW/m^2 using Lienhard's constant ($C_C = 0.149$),[14] 1.354 MW/m^2 using Kutateladze's constant ($C_C = 0.16$),[15] and 1.523 MW/m^2 using Rohsenow's constant ($C_C = 0.18$).[16] The prediction by the model of Haramura and Katto is well within the range of the previously correlated CHF data at atmospheric pressure. Unfortunately, similar assessment is not possible at higher pressures because macrolayer-thickness data at these pressures do not exist. Therefore, we extrapolated the data of Bhat *et al.*[5] by assuming that A_1/A_w follows the form suggested by Haramura and Katto.[7]

$$\frac{A_1}{A_w} = C_A \left(\frac{\rho_g}{\rho_f}\right)^{0.2} \quad , \tag{5}$$

where the constant C_A is evaluated at atmospheric pressure through the data of Bhat *et al.*,[5] which yields

$$7.17 \times 10^{-2} \le C_A \le 9.62 \times 10^{-2} \quad .$$

Figure 1 shows the comparison between the model of Haramura and Katto, where Eq. (5) is substituted into Eqs. (3) and (4), and the Zuber correlation with various constants. As shown in this figure, even when the macrolayer-thickness data of Bhat *et al.* are extrapolated to higher pressures, the agreement between the multistep model and the previously assessed correlations is quite favorable. Therefore, we believe that this section brings a further verification of the steady state CHF model of Haramura and Katto, which constitutes the kernel of our transient CHF model.

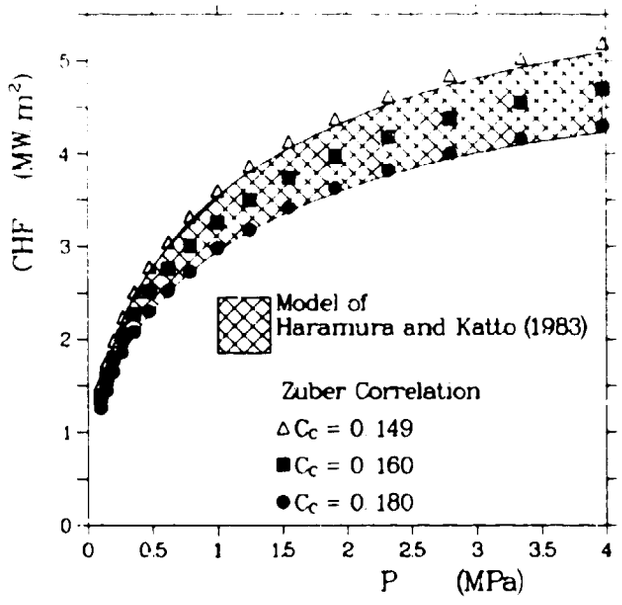

Fig. 1.
Comparison of the Zuber correlation with the model of Haramura and Katto.

III. EFFECT OF THE HEATER'S THERMAL STORAGE ON THE TRANSIENT CHF MODEL

In our previous study,[1] when we compared the transient CHF model given by Eq. (1) with the data of Sakurai and Shiotsu,[5] we assumed that the surface heat flux between $t_{CHF,SS}$ and $t_{CHF,TR}$ may be related to the exponential heat generation rate as follows:

$$q(t) \quad \left(\frac{V}{S}\right) \cdot Q_1 \exp\left(\frac{t}{\tau}\right) , \tag{6}$$

where V and S are the heater volume and surface area, respectively. This assumption, which we refer to as the quasi-steady conduction model, yields an exponential increase in the surface heat flux where the exponential period is the same as the exponential period of the heat generation rate. With this assumption, the theory overpredicted the data at small exponential periods; however, the discrepancy was confined within 25%.

In this section, we calculate the conduction effect within the heater on the prediction of the transient CHF model. In order to calculate realistically the relationship between q and Q, we must either theoretically model the entire boiling curve or use the surface heat flux versus time data of Sakurai and Shiotsu to solve the transient conduction equation within the heater, from the start of the transient up to the inception of the transient CHF. The former is a difficult task, whereas the latter is not available in the open literature. Therefore, we decided to develop an approximate approach using the following assumptions.

1. First, we restricted our analysis to the transient CHF data where *regular boiling* occurs. Regular boiling is defined by Sakurai and Shiotsu[4] as transient boiling where the transient nucleate boiling curve recovers the steady-state nucleate boiling curve before steady-state CHF and remains along the extension of the steady-state nucleate boiling curve until it reaches the transient CHF. Regular and irregular boiling curves are shown in Fig. 2. Figure 3 shows the boiling pattern map for the experiments of Sakurai and Shiotsu.[5] In their experiment, Sakurai and Shiotsu observed that regular boiling occurs with exponential periods greater than 5 ms at pressures greater than 0.588 MPa. Because the fastest transient CHF measurements correspond to an exponential period of 5 ms, we restricted the analysis in this paper to the data at pressures greater than 0.588 MPa. With this restriction, we are able to approximate the surface heat flux/surface temperature relation between the times $t_{CHF,SS}$ and $t_{CHF,TR}$ through the use of an appropriate steady-state nucleate boiling correlation, such as the Rohsenow correlation.[16]
2. We also assumed that, between $t_{CHF,SS}$ and $t_{CHF,TR}$, the surface heat flux increases exponentially such that

$$q(t) = q_{CHF,SS} \exp\left(\frac{t}{\tau^*}\right) , \tag{7}$$

where $q_{CHF,SS} \le q(t) \le q_{CHF,TR}$ and $\tau^* \ge \tau$.

3. Finally, we assumed that the temperature profile remains parabolic in shape between $t_{CHF,SS}$ and $t_{CHF,TR}$. Although we know that the real temperature profile is time-dependent, this assumption allows us to see the effect of temperature profile upon the results. Thus,

$$T(t,r) \quad T_w(t) \cdot \frac{q(t)d}{4k_h}\left(1 \quad \frac{r^2}{R^2}\right) . \tag{8}$$

The instantaneous average temperature then can be calculated as

$$T_a(t) \quad T_w(t) \cdot \frac{q(t)d}{8k_h} . \tag{9}$$

Between $t_{CHF,SS}$ and $t_{CHF,TR}$, the total heat generated per unit volume for an exponential power transient is given by

$$Q_{total} \quad \int_{0}^{t_{CHF,TR}} Q_{CHF,SS} \exp\left(\frac{t'}{\tau}\right) dt' , \tag{10}$$

where $t' \quad t \quad t_{CHF,SS}$. Equation (10) can be approximated by the following expression.

$$Q_{total} \quad \frac{4q_{CHF,SS}\tau}{d}\left|\exp\left(\frac{t_{CHF,TR}}{\tau}\right) \quad 1\right| . \tag{11}$$

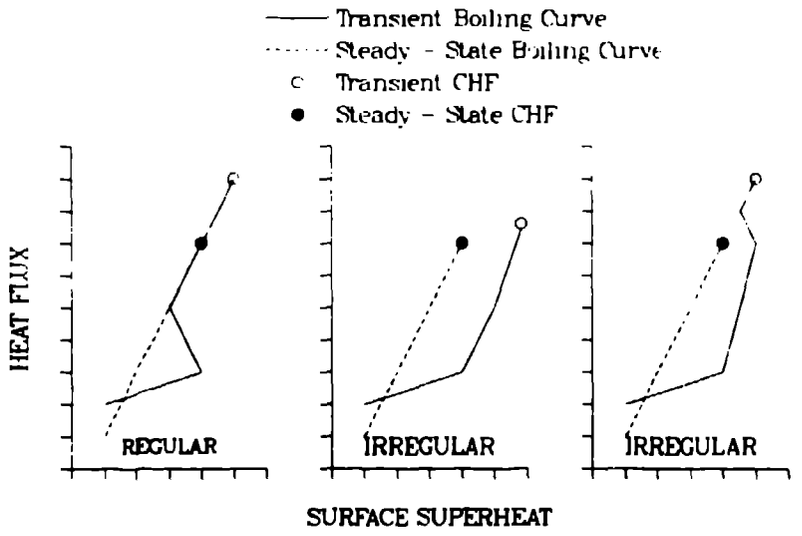

Fig. 2.
Transient nucleate boiling map for the experimental setup of Sakurai and Shiotsu.[4,5]

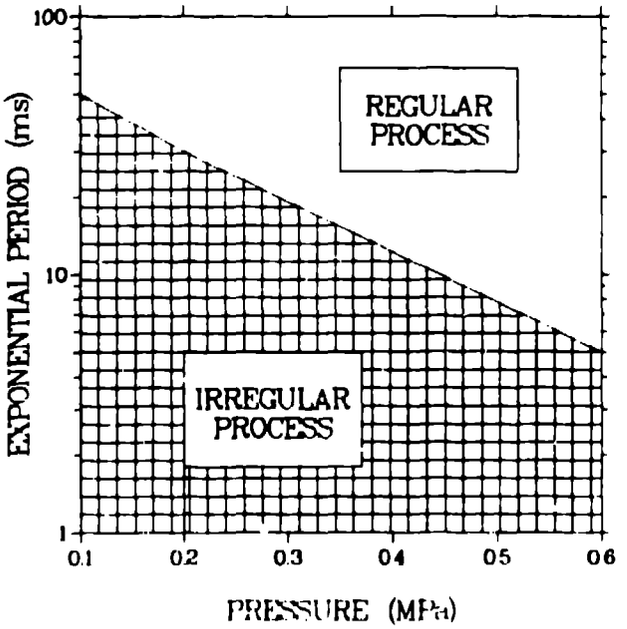

Fig. 3.
Different transient boiling curves.

The total heat stored per unit volume within the heater is given by

$$Q_{\text{stored}} = \rho_h C_h (T_{a,\text{CHF,TR}} - T_{a,\text{CHF,SS}}) \quad . \tag{12}$$

where $T_{a,\text{CHF,TR}} - T_{a,\text{CHF,SS}}$ may be calculated using Eq. (9) as follows.

$$T_{a,\text{CHF,TR}} - T_{a,\text{CHF,SS}} = T_{w,\text{CHF,TR}} - T_{w,\text{CHF,SS}} + \left[\frac{(q_{\text{CHF,TR}} - q_{\text{CHF,SS}})d}{8k_h}\right] \quad . \tag{13}$$

Note that the first term within the first set of brackets on the right-hand side (RHS) of Eq. (13) corresponds to a lumped system. Near CHF, the calculated Biot number is on the order of unity for a platinum heater with a 1.2-mm diameter. Therefore, the system is not lumped and the second term on the RHS must not be neglected. Because our analysis is restricted to regular boiling, the relationship between the heat flux and the surface temperature can be found using a nucleate boiling correlation such as the one given by Rohsenow[16] as

$$\frac{C_f(T_w - T_{\text{sat}})}{h_{fg}} = C_B \left(\frac{qL_c}{\mu_f h_{fg}}\right)^{0.33} \left(\frac{C_f \mu_f}{k_f}\right) \quad , \tag{14}$$

where C_B is 0.013 for platinum heaters in water and L_c is the Laplace coefficient given by

$$L_c = \left[\frac{\sigma}{g(\rho_f - \rho_g)}\right]^{1/2} \quad .$$

Equation (14) can be written in the form,

$$T_w - T_{\text{sat}} = \phi(P) \cdot q^{0.33} \quad , \tag{15}$$

where

$$\phi(P) = 0.013 \left(\frac{L_c}{\mu_f h_{fg}}\right)^{0.33} \left(\frac{h_{fg}\mu_f}{k_f}\right) \quad . \tag{16}$$

Thus, by substituting Eqs. (13) and (15) into Eq. (12), the heat stored per unit volume may be calculated as

$$Q_{\text{stored}} = \rho_h C_h \phi (q_{\text{CHF,TR}}^{0.33} - q_{\text{CHF,SS}}^{0.33}) - \frac{d}{8\alpha_h}(q_{\text{CHF,TR}} - q_{\text{CHF,SS}}) \quad . \tag{17}$$

Finally, the total heat convected to the fluid per unit heater volume is given by

$$Q_{\text{convected}} = \int_0^{t_{\text{CHF,TR}}} \frac{4}{d} q_{\text{CHF,SS}} \exp\left(\frac{t}{\tau}\right) dt = \frac{4q_{\text{CHF,SS}}}{d}\tau \left[\exp\left(\frac{t_{\text{CHF,TR}}}{\tau}\right) - 1\right] \quad . \tag{18}$$

Substituting Eqs. (11), (17), and (18) into the energy balance where

$$Q_{\text{total}} \quad Q_{\text{stored}} - Q_{\text{convected}}$$

and rearranging the terms, we obtain

$$\left[\eta^{1.5}\tau^{*} - \tau^{*} - 1\right] = \frac{\tau^{*}}{\tau}(\eta \quad 1) \quad \frac{\rho_h C_{\cdot\cdot} d}{4q_{\text{CHF SS}}\tau}(\eta^{0.33} - 1) - \frac{d^2}{32\alpha_h \tau}(\eta - 1) \quad . \qquad (19)$$

Equations (1) and (19) constitute a set of two equations with two unknowns (η and τ^{*}) that must be solved simultaneously. For the experimental conditions of Sakurai and Shiotsu[4,5] that yield regular boiling, the numerical solutions are shown in Figs. 4–6.

Figure 4 illustrates the relation between τ and τ^{*} for a platinum wire with a 1.2-mm diameter placed in a pool of saturated water at various pressures. As expected, τ^{*} is considerably greater than τ for small values of τ, whereas the difference decreases as τ increases. In the limit, as τ goes to infinity, Fig. 4 shows that τ^{*}/τ goes to 1.17. However, beyond $\tau = 1$ s, the quasi-steady conduction solution yields less than 1% error. Thus, the solution for the relationship of τ and τ^{*} beyond 1 s has no practical importance. Figures 5 and 6 show the comparison of Eq. (1) with the data of Sakurai and Shiotsu[5] at pressures of 2.056 and 1.079 MPa, respectively. The solutions with quasi-steady conduction ($\tau = \tau^{*}$), the lumped-system assumption, and the parabolic profile assumption are shown in these figures. As shown, the current transient CHF theory is improved considerably when it is coupled with the conduction solution using a parabolic profile. This approach, however, still contains certain approximations that will be discussed further in the last section of this paper.

IV. EFFECT OF THE RANDOM VAPOR MASS BEHAVIOR ON THE TRANSIENT CHF MODEL

In our previous study,[10] the magnitude of the transient CHF was treated as a deterministic value. However, during transient boiling, the history of a given vapor mass may affect the final prediction, and this effect suggests a statistical value for the transient CHF. Such statistical effects are expected to be rather weak because of the strong influence of the hydrodynamic-thinning mechanism during fast transients. This mechanism is effective regardless of the vapor mass behavior. During slower transients, the process becomes almost steady state. Therefore, the statistical effects also are expected to be small. Nevertheless, we quantified these effects for slow, fast, and very fast transients and evaluated the results through data comparison.

First, we consider the relatively slower transients. During such transients, the switch-over from hydrodynamic to thermal thinning occurs before the surface heat flux reaches $q_{\text{CHF,SS}}$. Therefore, even before steady-state CHF, the macrolayer thinning is dominated by evaporation during the vapor mass hovering period. In our previous study,[1] we characterized these transients based upon the magnitude of the switch-over parameter as B_s 1. The first term on the RHS of Eq. (1), which corresponds to slower transients, was obtained by assuming that either switch-over occurs or a new vapor mass is formed at t $t_{\text{CHF SS}}$. The calculated value does not correspond to either the minimum or maximum possible value of transient

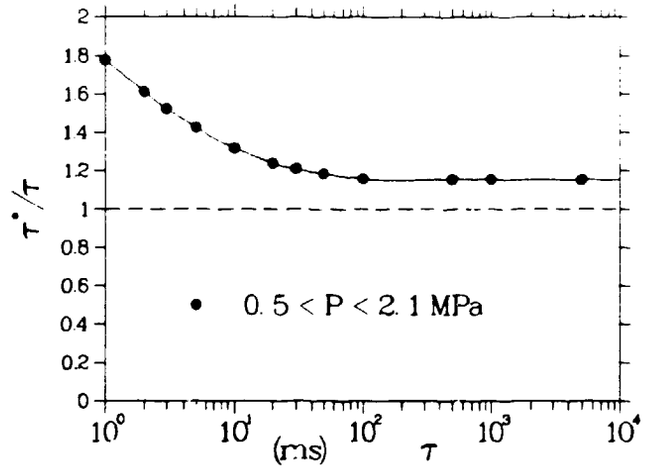

Fig. 4.
Relationship between τ^* and τ.

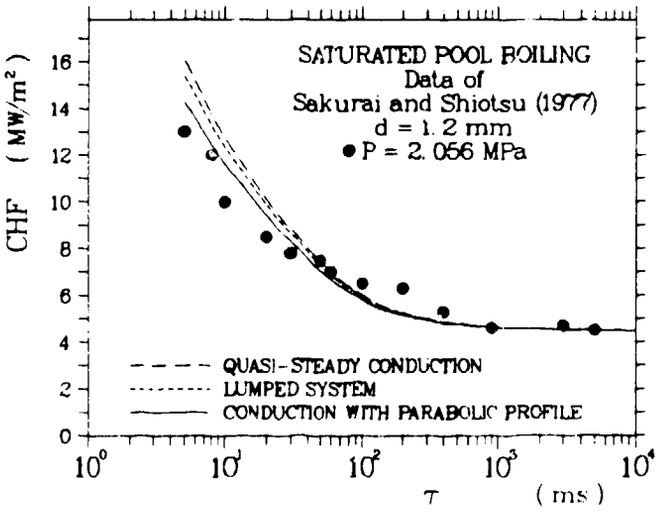

Fig. 5.
Comparison of the current theory with the data of Sakurai and Shiotsu[5] at 2.056 MPa using different conduction models.

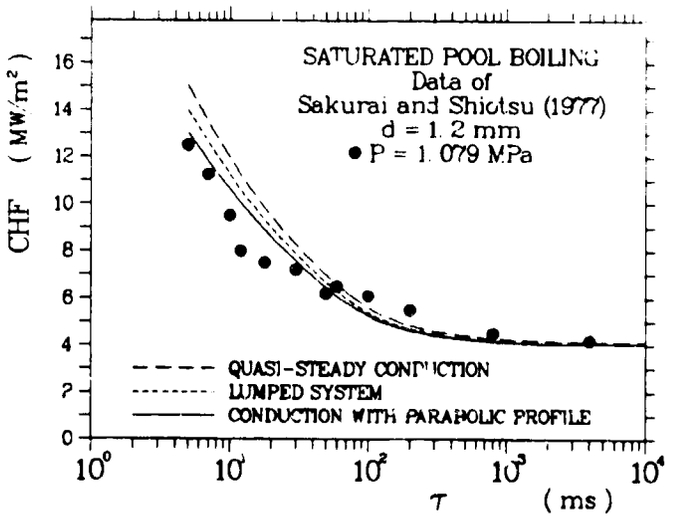

Fig. 6.
Comparison of the current theory with the data of Sakurai and Shiotsu[5] at 1.079 MPa using different conduction models.

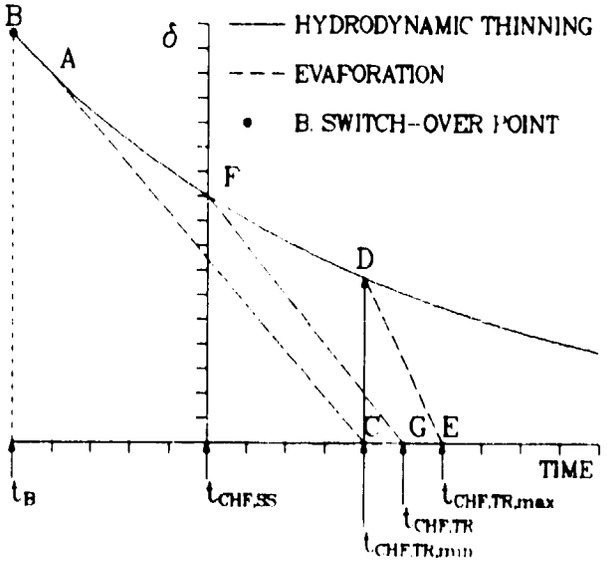

Fig. 7.
Schematic description of the macrolayer thinning mechanism during slow transients.

CHF but is used as an approximation between the maximum and minimum values. The corresponding macrolayer thickness follows the curve FG in Fig. 7.

To calculate the minimum possible value of transient CHF, we assume that a vapor mass is formed at point A in Fig. 7, where $t_B = t_A = t_{CHF,SS}$. For the macrolayer underneath this vapor mass to dry out in an evaporation mode at time t_C, the energy deposition must be high enough to evaporate all the liquid during the vapor mass hovering period. Thus, the following inequality must be satisfied.

$$(\delta_c)_{q=q_A} \geq \int_0^{\eta^{1.5}\tau_d} \frac{q_A \exp\left(\frac{t^*}{\tau^*}\right)}{f_2} \, dt^* \quad , \tag{20}$$

where $t^* = t - t_A$ and

$$f_2 = \rho_g h_{fg} \left(1 - \frac{A_v}{A_w}\right) \quad .$$

The term $\eta^{1/5}\tau_d$ in Eq. (20) represents the vapor mass hovering period when the surface heat flux is equal to $q_{CHF,TR}$. As we showed in an earlier study,[17] during transient boiling the vapor mass hovering period is almost independent of history effects and may be calculated as a function of the departure heat flux using a steady heat flux model. Using Eq. (3) and the fact that the critical liquid-layer thickness is inversely proportional to q^2, the inequality in Eq. (20) yields

$$q_A \geq B_s q_{CHF,SS} \left\{ \frac{1}{2\left[\exp\left(\frac{\eta^{1.5} B_s^2}{2}\right) - 1\right]} \right\}^{1/3} \quad . \tag{21}$$

Because our analysis is concerned with slower transients where $B_s = 1$ and $\eta = 1.5$, we can safely approximate $\eta^{1.5}$ by 1. Thus, when the terms are rearranged, we obtain

$$\eta_{min} \geq B_s \exp\left(\frac{B_s^2}{2}\right) \left\{ \frac{1}{2\left[\exp\left(\frac{B_s^2}{2}\right) - 1\right]} \right\}^{1/3} \quad . \tag{22}$$

This result is valid only for slow transients where dryout under a given vapor mass occurs because of evaporation alone during its hovering period. Therefore, q_A must be greater than or equal to the switch-over heat flux q_H, which is defined as $B_s q_{CHF,SS}$. Thus, Eq. (21) yields

$$\left\{ \frac{1}{2\left[\exp\left(\frac{B_s^2}{2}\right) - 1\right]} \right\}^{1/3} \geq 1 \quad . \tag{23}$$

The solution of this inequality yields

$$B_s \geq 0.93 \quad .$$

Therefore, the vapor mass that can lead to the earliest dryout must be formed when $q = 0.93\ q_{CHF,SS}$. Any vapor mass formed earlier will depart before dryout, whereas the vapor masses formed after will lead to dryout before their departure.

The maximum possible value of transient CHF, for the same slow transient, corresponds to the case where the vapor mass departs before the dryout (at point C), and fresh liquid replenishes the macrolayer. Thus, the macrolayer follows the path ACDE. The corresponding maximum transient CHF may be obtained through the solution of the following integral.

$$(\delta_c)_{q=q_{CHF,TR,min}} = \int_0^{t'_{CHF,TR,max}} \frac{q_{CHF,TR,min} \exp\left(\frac{t'}{\tau}\right)}{f_2}\, dt' \quad , \tag{24}$$

where $t' = t - t_{CHF,TR,min}$. Rearranging the terms in Eq. (24) yields

$$\eta_{max} = \eta_{min} + \frac{B_s^2}{2\eta_{min}^2} \quad , \tag{25}$$

where η_{min} is given by Eq. (22).

During faster transients ($B_s \geq 0.93$), the macrolayer thinning under the vapor mass leading to the earliest possible dryout is caused partially by hydrodynamic thinning. For these transients, the macrolayer-thickness history in the vicinity of transient CHF is shown in Fig. 8. A vapor mass initiated after the switch-over point will lead to dryout, whereas a vapor mass initiated before the switch-over point may depart before dryout (point C). As shown in Fig. 8, the behavior of the vapor mass before the switch-over point ($t < t_B$) does not affect the liquid-layer thickness. The only time the macrolayer thickness is affected by the vapor mass departure is when this departure occurs after the switch-over time. Therefore, what we previously postulated to be $t_{CHF,TR}$ actually applies if the vapor masses do not depart between t_B and $t_{CHF,TR}$. Thus, the transient CHF (or η) calculated through this approach must be considered to be the minimum possible magnitude and is denoted as η_{min}, which is given by the second term on the RHS of Eq. (1). Thus, for fast transients,

$$\eta_{min} = 1.53 B_s \quad . \tag{26}$$

The maximum possible value corresponds to the case where the vapor mass departs just before dryout ($t < t_{CHF,TR,min}$). Thus, the liquid-layer thickness follows the path ABCDE in Fig. 8. Through an analysis similar to that for slow transients, we can show that the maximum heat flux also is given by Eq. (25), where η_{min} must be obtained from Eq. (26).

We also must remember that the above analysis is not applicable to very fast transients. If the transient is fast enough that the very first vapor mass that forms remains on the surface until the transient CHF occurs, the transient CHF becomes a deterministic rather than a probabilistic value. Actually, in these cases, it is more appropriate to talk about a vapor blanket overlaying the macrolayer rather than vapor masses because without departure

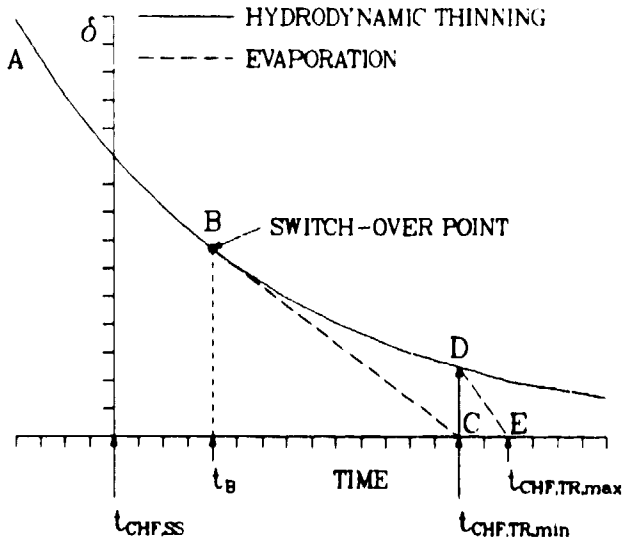

Fig. 8.
Schematic description of the macrolayer-thinning mechanism during fast transients.

the Taylor wave pattern for individual vapor masses may not be distinguished. Such rapid transients correspond to the case where

$$\frac{q_{CHF,TR}}{q_{M\ B}} \cdot \exp\left(\frac{\eta^{1.5}\tau_d}{\tau^*}\right) \quad . \tag{27}$$

In Eq. (27), $q_{M\ B}$ represents the heat flux corresponding to the first transition point on the boiling curve as formulated by Moissis and Berenson.[18] Even though, during transient boiling, the first transition may occur at a heat flux lower than what is predicted by the correlation of Moissis and Berenson because of the temperature overshoot at the early stages of the transient, their correlation may be used as a first-order analysis. At pressures between 1 and 2 MPa, the ratio $q_{CHF,SS}/q_{M\ B}$ is approximately equal to 10. At the same pressures and for a horizontal wire with a 1.2-mm diameter, the hovering period when $q \quad q_{CHF,SS}$ (denoted as τ_d) is approximately 30 ms. After substitution into Eq. (27), we obtain

$$\frac{\tau^*}{30} \quad \frac{\eta^{1.5}}{\log(10\eta)} \tag{28}$$

The simultaneous solution of Eqs. (1) and (28) roughly recommends $\tau^* \cdot 10$ ms.

We can summarize this statistical analysis by the following expression.

$$\eta_{\min} = \{1 - H(B_e - 0.93)\} B_e \exp\left(\frac{B_e^2}{2}\right) \left\{ \frac{1}{2\left[\exp\left(\frac{B_e^2}{2}\right) - 1\right]} \right\}^{1/2} \cdot \{H(B_e - 0.93)\} 1.5 B_e \quad , \tag{29}$$

and

$$\eta_{\max} = \eta_{\min} + \frac{B_e^3}{2\eta_{\min}^2} \quad . \tag{30}$$

Figures 9 and 10 show the range covered by Eqs. (29) and (30) compared with the high-pressure data of Sakurai and Shiotsu.[5] As shown in these figures, the current theory that suggests small data scatter is in agreement with such scatter during slower transients. It also is worth noting that, if evaporation is assumed to be the only thinning mechanism as suggested by Serizawa,[9] the scatter for fast transients will be much larger. This assumption is contradicted by the experimental data.

V. SUMMARY AND CONCLUSIONS

In this paper, we evaluated some assumptions that we postulated for an earlier transient CHF model.[10] This transient model is based upon the steady-state CHF model of Haramura and Katto.[7] As a first step, we evaluated the model by incorporating the steady-state macrolayer-thickness data that recently have appeared in the literature. The results show excellent agreement with the commonly used CHF correlations.

To study our transient CHF model, we coupled it with the thermal conduction solution within the heater. Thermal storage within the heater was neglected in our previous study. The resulting improvement is shown in Figs. 5 and 6. The remaining discrepancy possibly is due to the following approximations required by the analysis.

1. The analysis was applied only to transients at high pressure where *regular boiling* occurs. Thus, between $t_{CHF,SS}$ and $t_{CHF,TR}$, the heat flux/surface temperature relationship is obtained from Rohsenow's nucleate boiling correlation that naturally has some errors associated with it.
2. Between $t_{CHF,SS}$ and $t_{CHF,TR}$, we assumed that an exponential increase in power generation rate yields an exponential increase in the surface heat flux with a different exponential period. Even though the heat flux is increasing monotonically with time, the accuracy of approximating such an increase by an exponential is questionable, especially for faster transients where the response of the individual bubble to any change on the wall becomes more important.
3. Between $t_{CHF,SS}$ and $t_{CHF,TR}$, we assumed that the temperature profile within the heater remains parabolic. This assumption improved the predictions as compared with lumped system predictions. Nevertheless, it is still inaccurate, especially for faster transients.

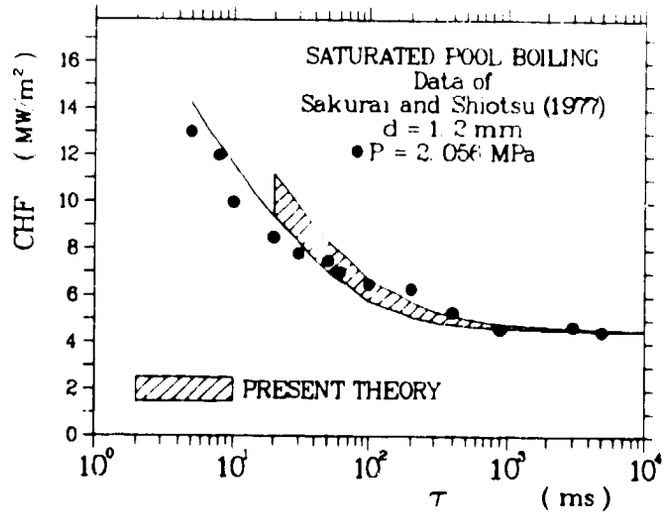

Fig. 9.
Comparison of the current theory with the data of Sakurai and Shiotsu[5] at 2.056 MPa including random vapor mass behavior.

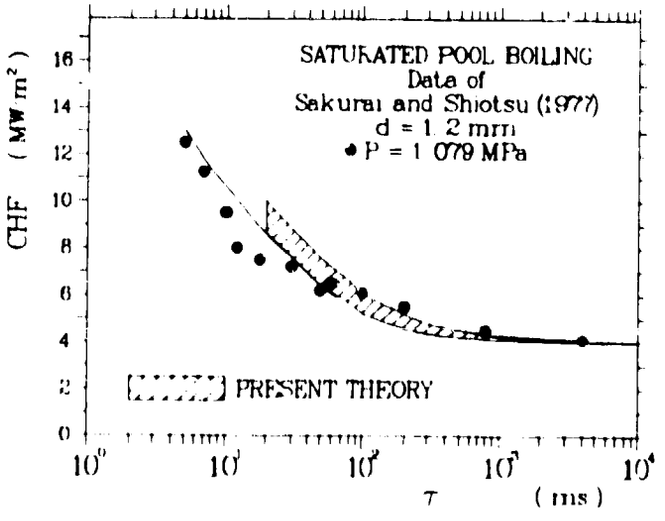

Fig. 10.
Comparison of the current theory with the data of Sakurai and Shiotsu[5] at 1.079 MPa including random vapor mass behavior

Unfortunately, we could not quantify the errors associated with these assumptions because surface temperature versus time and heat flux versus time data during transient CHF experiments are not reported in the open literature.

Finally, we analyzed the effect of random vapor mass behavior on the transient CHF model. Through this analysis, we obtained an envelope covering the possible values of transient CHF. As shown in Figs. 9 and 10, the range of this envelope is relatively small and it is in agreement with the small data scatter observed during transient CHF experiments. Figures 9 and 10 were generated by assuming a parabolic temperature profile within the heater. Therefore, the discrepancy for faster transients is expected. During slower transients, such statistical analysis improved the agreement between the theory and the data. The small data scatter also verifies the importance of the hydrodynamic thinning, without which the scatter would have been much larger during fast transients.

APPENDIX A

BUBBLE HOVERING PERIOD IN SATURATED POOL BOILING

In this appendix, the equation given by Haramura and Katto[7] to estimate the hovering period is summarized. This equation is obtained by solving the equation of motion for an idealized bubble.[19,20] Haramura and Katto[7] formulated the hovering period in the following form,

$$\tau_d = \left(\frac{3}{4\pi}\right)^{1/2} \left(\frac{4}{g}\right)^{1/3} \left(\frac{\xi\rho_f + \rho_g}{\rho_f - \rho_g}\right)^{1/3} v_1^{0.2} \quad , \qquad (A\ 1)$$

where v_1 is the volumetric growth rate of the vapor mass and ξ is the volumetric ratio of the accompanying liquid to the moving vapor mass. The term ξ is estimated theoretically as 11/16 by Haramura and Katto.[7]

The volumetric grow rate of the bubble is given by an energy balance as

$$v_1 = \frac{A_b q}{\rho_g h_{fg}} \quad , \qquad (A\ 2)$$

where A_b is the heater area contributing to one vapor mass and equal to λ_D^2, for a flat plate and $\pi d\lambda_D'$, for a horizontal wire with a small diameter. The parameter λ_D, the unstable Taylor wavelength, is given by

$$\lambda_D = 2\pi\sqrt{3}\left[\frac{\sigma}{g(\rho_f - \rho_g)}\right]^{1/2} \quad . \qquad (A\ 3)$$

For cylindrical heaters of small diameter, λ_D is modified to include the additional effect of the surface tension along the curvature and is given by

$$\lambda_D' = \frac{\lambda_D}{\sqrt{1 + 2\sigma/d^2 g(\rho_f - \rho_g)^{1/2}}} \quad . \qquad (A\ 4)$$

In the current study, the hovering period τ_d is estimated at a steady-state CHF level. Thus, q in Eq. (A 2) must be replaced by $q_{CHF,SS}$.

APPENDIX B

ZUBER CHF CORRELATION

The well known Zuber correlation is given by

$$\frac{q_{CHF,SS}}{\rho_g h_{fg}} = C_z \left[\frac{\sigma g(\rho_f - \rho_g)}{\rho^2}\right]^{1/4} \quad , \qquad (B\ 1)$$

where various values for the proportionality constant C_z have been suggested. Originally, Zuber[13] calculated C_z to be 0.131. It was later modified by Lienhard[14] to 0.149. Independently of Zuber, Kutateladze obtained Eq. (B 1) through dimensional analysis where C_z was suggested as 0.15 ± 0.03 through data comparison (as cited by Rohsenow[15]). Rohsenow suggests $C_z = 0.18$ must be used for the best data prediction.

REFERENCES

1. F. Tachibana, M. Akiyama, and H. Kawamura, "Heat Transfer and Critical Heat Flux in Transient Boiling (I)," *J. Nucl. Sci. Technol.* **5**, 117-126 (1968).
2. A. Sakurai, K. Mizukami, and M. Shiotsu, "Experimental Studies on Transient Boiling Heat Transfer and Burnout," in *Heat Transfer 1970* (Elsevier, Amsterdam, 1970), Vol. 5, paper B-3.4
3. H. Kawamura, F. Tachibana, and M. Akiyama, "Heat Transfer and DNB Heat Flux in Transient Boiling," in *Heat Transfer 1970* (Elsevier, Amsterdam, 1970), Vol. 5, paper B-3.3.
4. A. Sakurai and M. Shiotsu, "Transient Pool Boiling Heat Transfer, Part 1: Incipient Boiling Superheat," *J. Heat Transfer* **99**, 547-553 (1977).
5. A. Sakurai and M. Shiotsu, "Transient Pool Boiling Heat Transfer, Part 2: Boiling Heat Transfer and Burnout," *J. Heat Transfer* **99**, 554-560 (1977).
6. A. Serizawa, "Theoretical Prediction of Maximum Heat Flux in Power Transients," *Int. J. Heat Mass Transfer* **26**, 921-932 (1983).
7. Y. Haramura and Y. Katto, "A New Hydrodynamic Model of Critical Heat Flux, Applicable Widely to Both Pool and Forced Convection Boiling of Submerged Bodies in Saturated Liquids," *Int. J. Heat Mass Transfer* **26**, 389-399 (1983).
8. A. M. Bhat, J. S. Saini, and R. Prakash, "Role of Macrolayer Evaporation in Pool Boiling at High Heat Flux," *Int. J. Heat Mass Transfer* **29**, 1953-1961 (1986).
9. Y. Iida and K. Kobayasi, "Distribution of Void Fraction Above a Horizontal Heating Surface in Pool Boiling," *Bull. J.S.M.E.* **12**, 283-290 (1969).
10. K. O. Pasamehmetoglu, R. A. Nelson, and F. S. Gunnerson, "A Theoretical Prediction of Critical Heat Flux in Saturated Pool Boiling During Power Transients," in *Nonequilibrium Transport Phenomena* (ASME, New York, 1987), HTD-Vol. 77, pp. 57-64.
11. K. O. Pasamehmetoglu, "Transient Critical Heat Flux," Ph.D. dissertation, University of Central Florida, (also EIES report 86 87 1) (August 1986).
12. N. Zuber, "Stability of Boiling Heat Transfer," *Trans. ASME* **80**, 711-719 (1958).
13. K. O. Pasamehmetoglu and R. A. Nelson, "The Effect of Helmholtz Instability on the Macrolayer Thickness in Vapor Mushroom Region of Nucleate Pool Boiling," *Int. Comm. Heat Mass Transfer* **14**, 709-720 (1987).
14. J. H. Lienhard, *A Heat Transfer Textbook* (Prentice Hall, New York, 1981).
15. W. M. Rohsenow, "Boiling," in *Handbook of Heat Transfer*, W. M. Rohsenow and J. P. Hartnett, Eds. (McGraw Hill Publishing Company, New York, 1973), pp. (13-1), (13-75).
16. W. M. Rohsenow, "A Method of Correlating Heat Transfer Data for Surface Boiling of Liquids," *Trans. ASME* **74**, 969-978 (1952).

17. K. O. Pasamehmetoglu, R. A. Nelson, and F. S. Gunnerson, "Study of the Hovering Period and Bubble Size in Fully Developed Pool Nucleate Boiling of Saturated Liquid with a Time-Dependent Heat Source," in *Nonequilibrium Transport Phenomena* (ASME, New York, 1987), HTD-Vol. 77, pp. 39–45.

18. R. Moissis and P. J. Berenson, "On the Hydrodynamic Transition in Nucleate Boiling," *Trans. ASME, J. Heat Transfer* **85**, 221–229 (1963).

19. Y. Katto and S. Yokoya, "Behavior of a Vapor Mass in Saturated Nucleate and Transition Boiling," *Heat Transfer Jpn. Res.* **5**, 45–65 (1976).

20. Y. Katto and Y. Haramura, "Critical Heat Flux on Uniformly Heated Horizontal Cylinder in an Upward Cross-Flow of Saturated Liquid," *Int. J. Heat Mass Transfer* **26**, 1199–1205 (1983).

NOMENCLATURE

A_i	Heater area that contributes to one vapor mass (m^2)
A_v	Heater area covered by vapor (m^2)
A_w	Total heater area (m^2)
B_s	Switch-over parameter (dimensionless)
C	Specific heat (J/kg)
C_A	Empirical constant in Eq. (5) (dimensionless)
C_B	Empirical constant of Rohsenow's nucleate boiling correlation (dimensionless)
C_C	Constant in Zuber CHF correlation (dimensionless)
d	Diameter (m)
f_2	Prescribed functions of pressure
g	Gravitational constant (m/s^2)
$H(\ )$	Heavy-side step function
h_{fg}	Latent heat of vaporization (J/kg)
k	Thermal conductivity (W/m · K)
L_c	Laplace coefficient (m)
P	Pressure (MPa)
Q	Power generation rate (W/m^3)
q	Surface heat flux (W/m^2)
q_{MIB}	Heat flux at the first transition point predicted by Moissis-Berenson correlation (W/m^2)
R	Heater radius (m)
r	Radial coordinate (m)
S	Total surface area of the heater (m^2)
T	Temperature (K)
t	Time (s)
V	Total volume of the heater (m^3)
v_1	Volumetric growth rate of the vapor mass (m^3/s)
α	Thermal diffusivity (m^2/s)
δ	Liquid layer thickness (m)

δ_c	Critical liquid-layer thickness determined by hydrodynamic instability (m)
$\delta_{c,ss}$	Critical liquid-layer thickness at steady-state CHF (m)
$\phi(P)$	Prescribed function of pressure
λ_H	Helmholtz unstable wavelength (m)
λ_T	Taylor unstable wavelength (m)
λ'_T	Modified Taylor unstable wavelength (m)
ξ	Volumetric ratio of the accompanying liquid to the moving bubble (dimensionless)
η	Ratio of transient CHF to steady-state CHF (dimensionless)
σ	Surface tension (N/m)
ρ	Density (kg/m^3)
τ	Exponential period of the power generation rate (s)
τ^*	Exponential period of the surface heat flux (s)
τ_d	Hovering period (s)
μ	Dynamic viscosity (Pa · s)

Subscripts:

a	Average
CHF	Critical heat flux
f	Saturated liquid
g	Saturated vapor
h	Heater
i	Initial value
max	Maximum possible value
min	Minimum possible value
sat	Saturation
SS	Steady state
TR	Transient
w	Wall condition